Title
Expression of Acyl-CoA wax-alcohol acyltransferase 2 (AWAT2) by human and rabbit meibomian glands and meibocytes.

Authors
Rho, Chang
Kim, Sun
Lane, Shelley
et al.

Publication Date
2022

DOI
10.1016/j.jtos.2021.11.010

Peer reviewed

HHS Public Access

Author manuscript

Ocul Surf. Author manuscript; available in PMC 2023 August 01.

Published in final edited form as:

Ocul Surf. 2022 January ; 23: 60–70. doi:10.1016/j.jtos.2021.11.010.

Expression of Acyl-CoA wax-alcohol acyltransferase 2 (AWAT2) by human and rabbit meibomian glands and meibocytes

Chang Rae Rho[a,b,c], **Sun Woong Kim**[a,d], **Shelley Lane**[a], **Fangyuna Gao**[e], **Jinseor Kim**[a], **Yilu Xie**[a], **Donald J. Brown**[a], **Dorota Skowronska-Krawczyk**[e], **James V. Jester**[a,*]

[a]Gavin Herbert Eye Institute, University of California, Irvine, Irvine, CA, USA

[b]Department of Ophthalmology, Daejeon St. Mary's Hospital, College of Medicine, The Catholic University of Korea, Daejeon, Republic of Korea

[c]Seoul St.Mary's Eye Hospital, Suwon, Republic of Korea

[d]Department of Ophthalmology, Yonsei University Wonju College of Medicine, Wonju, Republic of Korea

[e]Department of Physiology and Biophysics, Department of Ophthalmology, Center for Translational Vision Research, School of Medicine, UC Irvine, Irvine, CA, USA

Abstract

Purpose: Previously, we showed that Acyl-CoA wax-alcohol acyltransferase 2 (AWAT2), an essential enzyme required for meibum wax ester synthesis, was not expressed by immortalized human meibomian gland epithelial cells (hMGEC) in culture. To begin to understand the mechanisms controlling AWAT2 expression, we have analyzed its expression in human and rabbit meibomian glands and cultured meibocytes.

Methods: Rabbit meibocyte progenitor cells (rMPC) were first grown in Cnt-BM.1 basal medium (Cellntec) supplemented with rhEGF, FGF10, and ROCK inhibitor (Y-27632 dihydrochloride), and then passed at 70–80% confluency with Accutase. Differentiation of rMPC to meibocytes (rMC) was induced by removal of Y-27632 and addition of 1 mM calcium with and without PPARγ agonists. RNA from the tissue, primary, passaged rMPC and differentiated rMC were obtained for AWAT2 qPCR analysis. Proteins and cells were evaluated for western blotting and neutral lipid synthesis, respectively. For comparison, human meibomian glands were separated for RNA and protein analysis. hMGEC was cultured to collect RNA and protein.

Results: Rabbit rMPCs were successfully grown, passaged, and differentiated, showing a significant increase in lipid droplet accumulation. AWAT2 RNA was highly expressed in tissue but showed a −16.9 log2 fold decrease in primary and passaged rMPCs and was not induced

*Corresponding author. 843 Health Sciences Road, University of California Irvine, Irvine, CA, 92697-4390, USA. jjester@uci.edu (J.V. Jester).

Declaration of competing interest

None.

Appendix A. Supplementary data

Supplementary data to this article can be found online at https://doi.org/10.1016/j.jtos.2021.11.010.

by differentiation to rMC. By comparison, human meibomian glands showed high expression of AWAT2, and hMGEC expressed non-detectable levels of AWAT2 transcripts or protein.

Conclusions: AWAT2 expression is lost in cultured rMPC and rMC suggesting that cells in culture do not undergo complete meibocyte differentiation and require yet to be identified culture conditions.

Keywords

Meibomian gland; Meibocyte; AWAT2; Cell culture; Rabbit

1. Introduction

Meibomian glands are holocrine secretory glands whose orifice at the eyelid margin connects a main central duct to individual acini that contain self-renewing acinar cells or meibocytes that synthesize meibum lipids [1]. Meibum is thought to play an important role in stabilizing the tear film to prevent aqueous tear evaporation, and meibomian gland dysfunction (MGD) either through synthesis of altered lipid quality or quantity or by dropout and atrophy of the meibomian gland has been shown to lead to excessive tear evaporation and an evaporative dry eye disease (DED) [2–5]. While considerable success has been made on characterizing the specific lipid species synthesized by the meibomian gland and how they control tear film stability and tear evaporation [6–8], the cellular and molecular mechanisms that control meibomian gland function are less understood. For the most part, recent studies have used an immortalized human meibomian gland epithelial cell line (hMGEC) to reveal underlying mechanisms that might regulate lipid/meibum synthesis by the meibomian gland acinar cells or meibocytes [9–11]. However, the suitability of this cell line for studying meibocyte differentiation and lipid synthesis has recently come under question.

Although the composition of meibum is complex, it is known that the characteristics of meibum lipid is different from the lipid produced in other human cells and tissues, even from sebum. One of the main differences is that meibomian lipids contain predominantly wax ester (WE), cholesteryl ester (CE), and cholesteryl (O)-acylated ω-hydroxy fatty acids (OAHFA), with WE reported to comprise 41% of the total lipids in human meibum [12,13]. Recently, acyl-CoA wax-alcohol acyltransferase 2 (AWAT2) has been shown to be critical to the synthesis of WE and knockout of this enzyme leads to a loss of meibum WE, an increase in the meibum melting point leading to increased viscosity and a dry eye phenotype [14,15]. Previous studies of human and mouse have identified AWAT2 as one of the most highly expressed enzymes associated with lipid synthesis in the meibomian gland and is therefore a potential biomarker for meibocyte differentiation [6,16]. However, in our studies of the molecular mechanisms of meibocyte differentiation using hMGEC, we could not detect the expression of AWAT2 in hMGEC when induced to differentiate and synthesize lipid using the peroxisome proliferator activated receptor gamma (PPARγ) agonist, rosiglitazone [17]. This finding was consistent with the finding by Hampel et al. that showed that WE synthesized from serum stimulated hMGEC comprised only 0.4–0.5% of the total lipids while CE comprised over 5% of the total lipids [18]. More recent findings by Ziemanski et al., could not even detect WE from serum stimulated hMGEC, in contrast to the long chain

CE [19]. Taken together, these findings question the utility of using hMGEC to probe the molecular mechanism controlling lipid synthesis by the meibomian gland.

To address this question, we have evaluated AWAT2 expression in both the rabbit meibomian gland and primary cultured rabbit meibocytes. Rabbit meibocytes were used in this study as they have been previously shown to undergo clonal expansion and differentiation in culture [20], as well as synthesize WE at a lower relative amount compared to human, ranging from 14 to 15% [21], though more recent studies have suggested that they synthesize only trace amounts [22]. While primary mouse meibocytes have also been studied [23], the number of mice required to perform these studies was deemed excessive. In this report we provide data confirming that AWAT2 is not detectable in differentiated hMGEC. Furthermore, while rabbit meibomian glands show high expression of AWAT2 RNA and protein in tissue, upon primary culture expression is rapidly lost for AWAT2 and is not elevated during meibocyte differentiation. Similarly, AWAT1 RNA and protein expression is high in tissues but lost in culture, albeit not to the same extent as AWAT2. Overall, these findings have two important implications. First, current cell culture methods used to study the molecular mechanisms controlling meibocyte differentiation do not adequately induce the expression of critical genes required for normal meibum synthesis, questioning the relevance of cell culture findings to normal meibomian gland function. Second, without an appropriate cell culture model that recapitulates meibocyte differentiation, gene expression and meibum lipid synthesis, it is not possible to confirm the cellular phenotype of immortalized cells currently used to study this process.

2. Methods

2.1. Human AWAT2 expression by meibomian glands and hMGEC

Human eyelid tissue, 1–2 days after death was obtained with permission from the University of California Irvine, Willed Body Program and consent of de-identified donors who provided tissue for scientific research. Eyelid tissue was then cut into 2 mm × 5 mm pieces containing the eyelid margin and tarsal plate and remaining, unused tissue was frozen and returned to the Willed Body Program for final disposition. Research tissue was then placed in Tissue Tech O.C.T. Compound (Sakura Finetek USA, Inc, Torrance, CA), snap frozen in liquid nitrogen and stored at −80 °C until cryo-sectioned for immunocytochemistry. Meibomian glands were also dissected from the tarsal plate and RNA and protein extracted for qPCR and western blotting, respectively. For hMGEC, cells were grown in Keratinocyte Serum Free Media (Invitrogen-Gibco, Grand Island, NY) as previously described [9]. At 80% confluency, cells were passaged onto collagen coated, 60 mm culture dishes and media changed to DMEM-F12 (Gibco, Grand Island, NY) containing EGF (10 ng/ml) and supplemented with either 10% fetal bovine serum (Sigma, St. Louis, MO) or rosiglitazone (30 μM, Sigma). Cells were then cultured for 7 days, and then RNA and protein collected for qPCR and western blotting as discussed below.

2.2. MALDI-TOF detection of rabbit WE

Meibomian gland wax ester identification and analysis was carried out using the method described by Butovich with a minor modification [24]. In brief, meibomian glands were

isolated from rabbit eyelids, cut into pieces, and homogenized with hexane. Crude extracts were evaporated almost to dryness and separated by thin-layer chromatography (TLC) with an eluent composition of chloroform: ethanol of 99:1. After separation, the separated wax esters were scraped from the TLC plate and extracted with hexane. The solvent was removed under a stream of nitrogen gas and the sample was dissolved in hexane for MALDI-TOF analysis. MALDI-TOF experiments were performed on a 5800 TOF/- TOF (AB Sciex, Framingham, MA, 01701, USA) operated in the reflectron mode. Data were collected and analyzed using AB SCIEX Analyst Software and Data Explorer. Samples dissolved were loaded on the MALDI plate using Ma/Sa technique: matrix (KDHB or LiDHB, synthesized by neutralization of DHB with LiOH or KOH) was spotted, after the solvent dried, the sample was applied on the top of the matrix and allowed to evaporate.

2.3. Isolation, culture, and passage of rabbit meibomian gland epithelial progenitor cells (rMPC)

Rabbit eyelids were obtained from Pel-Freez Biologicals (Rogers, AR). The upper and lower eyelids of five 8-week-old, New Zealand Albino rabbits were trimmed to remove redundant fat and connective tissue. Lids were washed with phosphate buffered saline (PBS, pH 7.2) and then placed in Dulbecco's modified Eagle's medium (DMEM) supplemented with Antibiotic Antimycotic Solution (Sigma, St Louis, MO). The conjunctiva and excess skin were then removed with Bard-Parker Blade #11 to isolate the tarsal plate (TP). TP was cut into small pieces with a sterile razor blade and then placed in DMEM containing 0.2% collagenase (Sigma, St Louis, MO) and 0.05% hyaluronidase (Sigma, St Louis, MO), digested at 37 °C 2 h, and then filtered through a 250 μm Tissue Strainer (Thermo Scientific, Rockford, IL) to remove large debris. The eluate was then filtered through a 40 μm pluiStrainer (PluiSelect, Germany) to remove single cells and retrieve larger, individual acini. The acini were suspended in CnT-BM.1 basal medium (Cellntec, Bern, Switzerland) supplemented with rhEGF (Gibco, Grand Island, NY), insulin-transferrin-selenium (Gibco, Grand Island, NY), FGF10 (Sino Biological, Wayne,PA), and the ROCK inhibitor, Y-27632 dihydrochloride (MCE, Monmouth Junction, NJ). Acini were cultured in collagen coated, T-75 culture flask and maintained in a humidified, 5% CO_2 incubator at 37 °C to grow primary rabbit meibocyte progenitor cells (rMPCs). The medium was changed every other day and cells were passaged at 70–80% confluency using Accutase (Innovative Cell Technologies, San Diego, CA). To determine the optimal concentration of Y-27632 for growth, P1 rabbit rMPCs were passed, seeded into 6 well plates, and grown in growth media supplemented with various concentrations of Y-27632 (0, 1, 5, 10, 20 and 30 μM). Phase contrast images were taken every 2 days and the cell numbers were counted to measure the change in cell density and cellular growth kinetics.

2.4. Differentiation and LipidTOX stain

Passaged rMPCs were induced to differentiate to meibocytes (rMCs) at 70–80% confluency. For the differentiation, CnT-BM.1 basal medium (Cellntec, Bern, Switzerland) containing rhEGF (Gibco, Grand Island, NY), insulin-transferrin-selenium (Gibco, Grand Island, NY), and FGF10 (Sino Biological, Wayne, PA) without the Y-27632 inhibitor was supplemented with calcium chloride (Promocell, Heidelberg, Germany) to make a final calcium concentration of 1.0 mM. To further induce meibocyte differentiation, 30 μM of

the PPARγ agonists, rosiglitazone (Sigma, St Louis, MO) was added to the media. Cells were then plated onto collagen coated glass coverslips and cultured for different times. Cells were then fixed in 2% paraformaldehyde in PBS and lipid content was measured by staining cells with the neutral lipid fluorescent probe, HCS LipidTOX ™ (Invitrogen, Carlsbad, CA) at 1:1000 dilution for 20 min at room temperature. Coverslips were rinsed in PBS, counterstained with DAPI nuclear stain and fluorescence images were taken using a Leica DMI6000B Epifluorescent microscope. A total of 3 random images for each coverslip (3 coverslips totaling 9 images per treatment) were digitized and then analyzed using Metamorph Image Processing Software (Molecular Devices, San Jose, CA, USA). All coverslips from each experiment were stained and evaluated on the same day to reduce the effects of random variations in staining intensity. Lipid content per cell was measured as described previously [23].

2.5. Immunocytochemistry

For analysis of intact meibomian glands, eyelids were obtained from 8-week-old rabbits (Pel Freez) within 24 h after death. Upon arrival at the lab, tissue was immediately dissected and then embedded in O.C.T. Compound, frozen in liquid nitrogen, and stored at −80 °C. Blocks were then sectioned using a Leica CM1850 Cryotome (Leica, Germany), and tissue sections mounted onto glass slides. For immunostaining, tissue sections were permeabilized in PBS containing 0.5% dimethyl sulfoxide and 0.5% Triton X (pH 7.2) for 5 min and then washed in PBS. Slides were then incubated in goat serum (1/30) for 30 min at 37 °C. Slides from human or rabbit eyelid were incubated with rabbit anti-DGAT2L4 antibody (1:50, Abcam Cat# ab204904, Cambridge, MA) or mouse anti-DGAT2L4 antibody (Sigma-Aldrich Cat# SAB1412930), respectively, washed with PBS, stained with FITC conjugated corresponding secondary IgG (1:200, Invitrogen) for 1 h at 37 °C, and then counterstained with DAPI (Invitrogen).

2.6. RNA isolation and analysis of AWAT1/2 gene expression

RNA was obtained from human tissue, cultured hMGEC, rabbit tissue, and primary, P1, P3, and P5 rMPCs and P2, P4, and P6 rMCs differentiated with 30 μM rosiglitazone for AWAT1/2 qPCR analysis. Briefly, RNA was isolated with the RNeasy Mini Kit following the manufacturer's instructions (Qiagen, Valencia, CA). RNA quantity and quality was determined with Nanodrop (Thermo Scientific, Wilmington, DE). Equal amounts of total RNA (1 μg) were reverse transcribed to obtain cDNA with the iScript Synthesis kit (Biorad, Germany) using the standard protocol. Real time PCR was performed using FastStart Essential DNA green master (Roche, Indianapolis, IN) with a Lightcycler® 96 system (Roche, Indianapolis, IN) and SYBR green real time PCR primers. Primers for RT-PCR were designed for human and rabbit (oryctolagus cuniculus) (Table 1). A three-step PCR protocol included an initial denaturation step (10 min 95 °C), 45 cycles of 15 s denaturation at 95 °C, 15 s annealing at 60 °C, and 45s extension at 72 °C followed by a melt gradient from 65 °C to 97 °C. PCR products were evaluated by melt curve analysis and sizing on agarose gels. Relative quantification for each condition was performed using the delta CT method. GAPDH and Actin were used as housekeeper genes.

2.7. Protein extraction and western blotting

Protein from tissues were extracted by first mincing the tissue using a PT1200 Polytron (Kinematica, Switzerland) in RIPA buffer. Cells in culture were lysed on ice using the Pro-prep™ protein extraction kit (Intron Biotechnology, Korea). Proteins (10–20 μg per lane) were then run on 10% polyacrylamide gels and proteins transferred to PVDF membranes (Invitrogen). Membranes were then blocked for 1 h in PBS containing 5% skim milk and 0.2% Tween-20 and then incubated overnight with primary antibodies to AWAT2 (H00158835–B01P, Abnova, Taiwan), SOX9 (Abcam, Cat# ab185966), P63 (Abcam, Cat# ab124762), and PCNA (Thermofisher, Cat# PA5-27214). Antibody-reactive proteins were detected with the appropriate HRP-conjugated secondary antibodies and an enhanced chemiluminescent substrate (SuperSignal West Pico Chemiluminescent Substrate, Thermos scientific). Immunostained bands were imaged and analyzed with ChemiDoc MP (Bio-Rad) and relative quantitation was done after normalization to GAPDH bands in the same blots.

2.8. Statistical analysis

All numeric results are reported as mean ± standard error. Differences between groups were assessed by Kruskal-Wallis one-way analysis of variance on ranks and Tukey all pairwise multiple comparison test (Sigma Stat version 3.11, Systat Software Inc, Point Richmond, CA). All experiments were repeated at least 3 times and a P value of <0.05 was regarded statistically significant.

3. Results

3.1. AWAT2 expression in human meibomian glands and hMGEC

Immunostaining of human meibomian glands with antibodies specific for AWAT2 showed strong staining of the acinar meibocytes (aM) and weak staining of the meibomian gland ductal epithelium (dEpi) (Fig. 1A). Additionally, AWAT2 was most prominently expressed in the suprabasal acinar meibocytes (Fig. 1C, inset), and was greatly reduced or not detected in basal acinar progenitor cells. Using the same antibody, protein extracted from the human eyelid tissue showed very high expression of AWAT2 in comparison to the expression of the house keeping gene, GAPDH (Fig. 1D). By comparison, protein isolated from hMGEC treated either with growth media (CTL) or DMEM/F12 supplemented with 10% fetal bovine serum (Serum) or 30 μM rosiglitazone (Rosi) showed little to no expression of AWAT2 detectable protein. Additionally, when RNA from human tissue and cultured hMGEC was probed for AWAT2 transcripts, there was over a 1600-fold higher level expression in eyelid tissue compared to GAPDH, while RNA extracted from control cells (CTL), serum treated cells (Serum) and rosiglitazone treated cells (Rosi) showed no detectable expression (Fig. 1E). Together these data show that human meibomian glands show very high expression of AWAT2, while the immortalized hMGEC fail to express AWAT2 under control or differentiation conditions.

3.2. AWAT2 expression in rabbit meibomian glands

To confirm that rabbit meibomian glands express AWAT2 and synthesized WE, we first immunostained rabbit eyelid tissue with antibodies to AWAT2. As was identified in

human eyelid tissue, rabbit meibomian glands showed staining for AWAT2 in the acinar compartment (Fig. 2A). Similar to human, rabbit acini appeared to show localization of AWAT2 to the suprabasal cell compartment that contained the differentiating meibocytes, and was not detected in the basal, meibocyte progenitor cell population (Fig. 2C, inset). Western blotting and PCR analysis were also consistent with the high expression of AWAT2, similar to that identified in human tissue (data not shown). To confirm that rabbit meibomian gland synthesized WE, we first performed a staining analysis of the meibum lipid components by TLC. As shown in Fig. 2D, the top band is wax esters, the bottom band is most likely to be free fatty acids, according to the retention factor order. The wax esters were then collected and analyzed by MALDI-TOF. As shown in Fig. 2E, the peaks were composed of a series of apparently related compounds with Δm/z values of 28n, similarly to wax esters in *Ginkgo biloba* leaves and beeswax [25]. The structure of WEs was further studied by MS/MS spectra. For example, F showed a MS/MS spectrum of $[M + Li]^+$ at *m/z* 431.3. The fragment was identified as lithium adduct of tetradecanoic acid (*m/z* 235.5). The alcoholic part of the WE was calculated from the mass difference between $[M + Li]^+$ and $[RCOOH + Li]^+$. Therefore, the structure of this particular WE was thus determined to be 14:0–14:0, the same as predicted.

3.3. Growth and differentiation of rabbit MPCs

Isolated individual rabbit acini were successfully grown on collagen coated culture dishes. As shown in Fig. 3A, rMPCs showed typical polygonal epithelial morphology and, using accutase, cells could be detached from the culture dish and passaged. We tested serial passage of rMPCs and confirmed that the cells were successfully grown and passaged up to P7, maintaining the typical polygonal epithelial morphology. Fig. 3B, C, and 3D shows P1, P5, and P7 cells, respectively. To determine the optimal concentration of ROCK inhibitor, Y-27632, used for stimulating proliferation of rMPCs, P2 cells were cultured in different concentrations of Y-27632 (Fig. 3E). rMPCs were confluent on day 9 using concentrations of both 10 and 20 μM, and 10 μM Y-27632 was chosen for growth conditions for the remaining experiments.

To differentiate rMPCs to rMCs, the basal CnT-BM.1 culture media was first modified by the removal of Y-27632 and the addition of 1.0 mM calcium (Ca++). To further induce meibocyte differentiation, the PPARγ agonist, rosiglitazone (Rosi) was also added to the culture medium at a concentration of 30 μM. To evaluate the effects of these different cell growth conditions, cells were grown, and then protein collected at different cell passages to assess cell proliferation as monitored by expression of PCNA, and maintenance of progenitor cell phenotype as identified by expression of SOX9 and p63 [26,27]. As shown in Fig. 4, expression of PCNA, SOX9, and P63 were all detected in rMPCs grown in basal media containing low calcium supplemented with Y-27632 at passages 1–5 (Fig. 4). However, removal of Y-27632 and addition of calcium significantly reduced PCNA and p63 expression ($P < 0.05$), while not effecting expression of SOX9 in passaged cells 1–5. However, the addition of rosiglitazone completely abolished expression of PCNA, suggesting complete cell cycle exit and cell differentiation. Additionally, SOX9 expression was significantly reduced compared to rMPCs and calcium treated cells ($P < 0.05$). Overall, these findings suggested that the CnT-BM.1 media supplemented with Y-27632 supported

a meibocyte progenitor cell phenotype, which is also maintained at a lower proliferative rate with the removal of Y-27632 and the addition of calcium. However, the addition of the PPARγ agonist, rosiglitazone, that has been shown to induce meibocyte differentiation and lipid synthesis [23,28,29], leads to further cell cycle exit and loss of the progenitor cell marker, SOX9.

To evaluate the potential of rMCs to synthesize lipid, rMPCs were plated on collagen coated glass coverslips and then cultured CnT-BM.1 media containing Y-27632 or media without Y-27632 and 1 μM Ca^{++} with and without rosiglitazone (30 μM). As shown in Fig. 5, rMPC grown in growth media and cells grown in differentiation media without rosiglitazone showed little or no accumulation of neutral lipid (A and B, respectively). However, when cells were treated with rosiglitazone, there was a dramatic increase in both the size and number of neutral lipid droplets (C). To evaluate the effect of cell passage on neutral lipid accumulation, Primary, P2, and P4 cells were passaged and grown in differentiation media with rosiglitazone for 6d. All passaged cells showed a significant increase of lipid droplets (Fig. 6A–C). Three parameters were measured including the lipid area (μm^2) per nuclei, droplet count per nuclei, and lipid area (μm^2) per droplet. All parameters were increased in P1 but showed decreasing levels of lipid synthesis at P3 and P5 (Fig. 6D–F).

3.4. Expression of AWAT2 in rMPCs and rMCs

Next, we evaluated expression of AWAT 1/2 genes using quantitative real time PCR for tissue, primary, P1, P3, and P5 cells in proliferation media and P2, P4, and P6 cells in differentiation media with rosiglitazone. Compared to tissue AWAT2 mRNA expression level, the mRNAs collected from rMPCs showed a dramatically decreased expression in both primary cultured cells and passaged cells at P1, P3, and P5. As shown in Fig. 7A, the log2 fold change of AWAT2 compared to tissue expression was −16.9, −18.0, −18.9, and −18.9 for primary, P1, P3, and P5 cells grown in CnT-BM.1 media containing Y-27632. Switching cells to differentiation media containing rosiglitazone showed no enhanced expression with levels continuing to be suppressed at −17.6, −17.0, and −19.1 log2 fold change of AWAT2 tissue expression levels for P2, P4, and P6 (Fig. 7B). These findings indicated that AWAT2 mRNA expression practically disappeared in 2D culture system even in primary cells. Also, the differentiation with rosiglitazone did not seem to affect the expression of AWAT2 mRNA and protein expression was undetectable (Fig. 7C).

When expression of AWAT1 was evaluated, the log2 fold change compared to tissue levels was −2.1, −2.4, −3.6, and −3.7 for primary, P1, P3, and P5 cells in proliferation media (Fig. 7A). When cells were differentiated with rosiglitazone, the log2 fold change of AWAT1 was −0.2, 0, and −3.0 for P2, P4, and P6 cells, respectively (Fig. 7B). These results suggest that rosiglitazone-induced rMPC differentiation moderately increased the AWAT1 mRNA expression in P2 and P4 cells, however this effect was not detected in P6 cells.

4. Discussion

This study reports two major findings. First, we confirm and extend earlier findings that have shown that the human meibomian glands highly express AWAT2, a critical enzyme that catalyzes the formation of WE from very long chain fatty acids and fatty alcohol

[30]. Furthermore, this expression appears localized to differentiating, suprabasal, acinar meibocytes and is not detectable in basal, meibocyte progenitor cells. We also confirm that hMGEC do not express detectable amounts of AWAT2 transcripts or protein under established culture conditions that promote growth or differentiation using either fetal bovine serum or PPARγ agonists. Secondly, using a rabbit meibocyte progenitor cell culture system, we establish that expression of AWAT2 is dramatically lost and undetectable even in primary cultured rMPCs. Further, AWAT2 expression remains undetectable following treatment with PPARγ agonists that induce features of meibocyte differentiation including, cell cycle exit, loss of progenitor cell markers, and accumulation of neutral lipid. The significance of these findings is discussed below.

4.1. Importance of AWAT2 expression to meibomian gland dysfunction and DED

As has been recently shown, expression of AWAT2 is critical for the synthesis of WE, and loss of this enzyme in transgenic mice leads to an increase in the melting point of meibum from 34 °C to 62 °C, resulting in marked thickening of meibum, retention within the central duct, and central duct dilation; all clinical signs of obstructive MGD [14,15]. Furthermore, recent studies of meibum lipid composition suggest that changes in cholesterol ester/wax ester ratios may affect the phase transition temperature of meibum making it more viscous in DED subjects and impairing lipid spreading over the ocular surface [7]. These changes, at least in the AWAT2 knockout mouse, can lead to disruption of the tear film and an evaporative dry eye phenotype [14,15]. Therefore, these findings strongly suggest that understanding the cellular and molecular regulation of AWAT2 expression and the control of WE synthesis in relation to the synthesis of other meibum lipids is not only important to understanding the role of meibum in stabilizing the tear film, but also to our understanding the pathogenesis of MGD.

To understand the regulation of meibum synthesis, studies have focused on the use of the hMGEC to probe the physiology and pathophysiology of the meibomian gland [9]. These studies have suggested that lipid production was increased with serum, omega 3 fatty acids, insulin, azithromycin, and IL-4 [11,18,31–33]. Rosiglitazone promoted upregulation of saturated and monounsaturated cholesteryl esters [34]. Androgen exposure decreased proinflammatory gene expression in hMGEC [35]. Drugs for dry eye disease including cyclosporin A, interleukin-1 receptor antagonist, P2Y2 receptor agonist, and rebamipide were tested on hMGEC. All these drugs showed no effect on cell proliferation and lipid accumulation. The drugs did not affect the expression of triglycerides, free cholesterol, or phospholipids in hMGEC [36].

However, concerns have been raised regarding the validity of using the hMGEC to study the meibomian gland pathophysiology. First, previously reported lipidomics of hMGEC showed only 0.5 or 0.4% of wax ester in total lipids under serum treatment [18], suggesting that culture of hMGEC under established culture conditions do not induce normal meibocyte differentiation and meibum lipid synthesis. Second, in our previous reports on the RNA analysis of hMGEC, transcripts for AWAT2 were not detectable in differentiated hMGEC as well as in control hMGEC [17]. Third, the growth medium requires BPE for cell proliferation and serum for its differentiation. The exact composition of the BPE and serum

is not known. This uncertainty makes it hard to understand the effect of the testing chemicals on the lipid synthesis. Last, the cell line was made from male donor. This poses a limit to the testing of hormonal effects within these cells and dry eye disease, which is known to be more prevalent in aged women.

In this study we establish that hMGEC under established culture conditions do not express or synthesize detectable amounts of AWAT2 transcripts or protein compared to that expressed by intact human meibomian glands. Importantly, we show that RNA transcripts for AWAT2 extracted from human eyelid tissue is over 1600-fold higher than that measured in cultured hMGEC. Furthermore, we were unable to detect any substantial increase in AWAT2 RNA or protein following treatment with either serum or rosiglitazone to induce lipid accumulation. While these findings explain earlier reports that hMGEC fail to synthesize WE, they also suggest that the conditions we currently use to grow and differentiate hMGEC are inadequate to induce meibocyte differentiation, either complete or in part. While this conclusion has been raised by other investigators [18], they remain of critical importance since findings from studies using hMGEC have the potential to impact clinical and therapeutic recommendations for treating MGD and DED.

4.2. Rabbit meibocyte progenitor cells and meibocyte differentiation

Like human and mouse [13], expression levels for AWAT2 RNA and protein in rabbit eyelids were found to be extremely high, showing strong positive immunostaining for AWAT2 in suprabasal meibomian gland acini. We have also grown acini isolated from the tarsus in matrigel three-dimensional culture for 3 days and identified continued strong AWAT2 expression in the acini as shown in Supplemental Fig. 1. However, as we show in this study, the RNA expression pattern was very different when the cells were grown in conventional two-dimensional culture system. Even in the primary cells grown from the isolated acini, the AWAT2 expression decreased more than 2^15 fold. Activation of PPAR-γ signaling pathway by rosiglitazone also had a negligible effect on the expression of AWAT2 in P2, P4, and P6 cells. While AWAT1 expression decreased in the primary cells, it was increased by rosiglitazone in P2 and 4 cells, but the augmenting effect vanished in P6. Further, these changes in AWAT1/2 expression pattern seemed unrelated to lipid droplet formation and accumulation. Even in the absence of the AWAT2, cultured cells produced numerous lipid droplets in P1, 3, and 5 in differentiation media with rosiglitazone. Thus, while isolated rMPCs can be induced to synthesize and accumulate lipid, these culture conditions are not sufficient to induce AWAT2 expression comparable to what is expressed in the intact meibomian gland.

Therefore, the observation that AWAT1/2 expression is lacking in cultured cells that accumulate lipid suggests that cells in culture do not undergo normal meibocyte differentiation. We speculate that lipid droplets in meibomian epithelial cells should not be assumed to be meibum considering the decrease in AWAT1/2 expression. Also, this raises the question on use of the conventional meibomian cell culture to test the meibomian gland physiology and pathology or the relevance of studying the effects of chemical and/or therapeutic agents on lipid accumulation in these cells.

4.3. Isolation and culture of rabbit meibocyte progenitor cells (rMPC)

To establish a culture of rMPCs, we adopted the use of a ROCK inhibitor and low calcium growth media that has been used in other epithelial cell cultures models. Previous reports have shown that rho kinase (ROCK) inhibitor, Y-27632, can inhibit terminal differentiation of cells in culture and increase cellular proliferation and passage of keratinocytes in vitro [37–39]. Low calcium media has also been shown to affect cellular differentiation and prolong the lifespan of basal primary keratinocytes by avoiding loss of basal cells [40]. Original culture of hMGEC used keratinocyte-serum free medium (SFM) whose calcium concentration below 0.1 mM maintains cell proliferation. Dulbecco's modified Eagle's medium and Ham's F12 supplemented with 10% FBS was then adopted for differentiation media as it contains 1.05 mM calcium [10,18]. In our approach, CnT-BM.1 media contained a very low calcium concentration (0.07 mM) to maintain basal cell proliferation and differentiation was then accomplished by removing the ROCK inhibitor and changing the calcium concentration to 1.0 mM, thus eliminating the need to switch to a different culture media.

Again, we also did not use serum or BPE in the media to address the uncertainties in FBS and BPE. FBS is known to contain various growth factors, hormones, and lipids with undetermined composition and concentration [41]. Here we tried to define and control all ingredients. The basal medium adopted is reported to have completely defined ingredients. We differentiated rMPCs to produce lipids by removing Y-27632 and adding calcium and rosiglitazone. The differentiation potential and lipid droplets were identified in P1, P3, and P5. Western blot analysis clearly showed that the differentiation medium strongly affected the cell's proliferating potential. PCNA and Sox9 were significantly decreased when cells were grown in media supplemented with both calcium and rosiglitazone.

5. Limitations

We have selected rabbit tissue primarily because of the ease of obtaining large quantities of eyelid tissue available through a food source abattoir compared to the purchase and sacrifice of very large numbers of mice that would have been required to collect sufficient meibomian glands for these studies. However, one lipidomics study of rabbit meibum noted that WE were only present in trace amounts. Furthermore, the overall profile of rabbit meibum appeared very different from that of human or mouse as well as the blink rate and presumed tear film stability [22]. Regarding the presence of WE in rabbit meibum it should be noted that much earlier studies of the rabbit meibum lipidome by Nicolaides et al., showed that WE comprised from 14 to 15% of the meibum lipids [21]. In this study, we have used Maldi-Tof to show that rabbit meibum does contain detectable amounts of WE, and that RNA and protein extracts from rabbit eyelid tissue contains abundant amounts of AWAT2, comparable to that identified in human eyelids. Furthermore, the immunolocalization of AWAT2 in rabbit meibomian gland acini appear similar to that of human and mouse (data not shown). While the differences between human and rabbit regarding the expression pattern of WE and other lipids may preclude the use of the rabbit to study human tear film function, it is our presumption that the rabbit meibocyte culture model can be used to understand the cellular and molecular mechanism controlling meibum lipid synthesis and the

relative presence of CE to WE synthesis. As with any animal model, our findings will need to be confirmed by studies using human meibocytes; however, the ability to obtain large numbers of cells for these experiments using rabbit eyelids may help in establishing culture conditions that could then be applied to human cells. In this regard, we conclude that the rabbit meibocyte culture model maybe extremely helpful, regardless of the different lipid species that are synthesized.

Another limitation concerns the culture conditions for the growth and differentiation of both hMGEC and rMPCs. For these studies we have used previously established and published protocol for hMGEC with some modifications. Furthermore, our study of rMPCs were limited to removal of the ROCK inhibitor and the addition of calcium with and without PPARγ agonists. It is likely that both conditions lack critical signals necessary for meibocyte differentiation. We therefore suggest that improvements in the culture model might help reveal critical signaling pathways necessary of meibocyte differentiation.

Supplementary Material

Refer to Web version on PubMed Central for supplementary material.

Funding

This work was supported in part by NIH/NEI EY021510, an Unrestricted Grant from Research to Prevent Blindness, Inc. RPB-203478, and the Skirball program in Molecular Ophthalmology and basic science research program through the National Research Foundation of Korea (NRF) funded by the Ministry of Education, Science and Technology (2020R1I1A3073515).

References

[1]. Jester JV, Nicolaides N, Smith RE. Meibomian gland studies: histologic and ultrastructural investigations. Invest Ophthalmol Vis Sci 1981;20:537–47. [PubMed: 7194327]

[2]. Foulks GN, Bron AJ. Meibomian gland dysfunction: a clinical scheme for description, diagnosis, classification, and grading. Ocul Surf 2003;1:107–26. [PubMed: 17075643]

[3]. Gilbard JP, Rossi SR, Heyda KG. Tear film and ocular surface changes after closure of the meibomian gland orifices in the rabbit. Ophthalmology 1989;96:1180–6. [PubMed: 2797721]

[4]. Mathers WD, Lane JA. Meibomian gland lipids, evaporation, and tear film stability. Adv Exp Med Biol 1998;438:349–60. [PubMed: 9634908]

[5]. Mishima S, Maurice DM. The oily layer of the tear film and evaporation from the corneal surface. Exp Eye Res 1961;1:39–45. [PubMed: 14474548]

[6]. Butovich IA. Meibomian glands, meibum, and meibogenesis. Exp Eye Res 2017;163:2–16. [PubMed: 28669846]

[7]. Hetman ZA, Borchman D. Concentration dependent cholesteryl-ester and wax-ester structural relationships and meibomian gland dysfunction. Biochem Biophys Rep 2020;21:100732. [PubMed: 32042930]

[8]. Sledge S, Henry C, Borchman D, Yappert MC, Bhola R, Ramasubramanian A, et al. Human meibum age, lipid-lipid interactions and lipid saturation in meibum from infants. Int J Mol Sci 2017;18. [PubMed: 29267212]

[9]. Liu S, Hatton MP, Khandelwal P, Sullivan DA. Culture, immortalization, and characterization of human meibomian gland epithelial cells. Invest Ophthalmol Vis Sci 2010;51:3993–4005. [PubMed: 20335607]

[10]. Liu S, Kam WR, Ding J, Hatton MP, Sullivan DA. Effect of growth factors on the proliferation and gene expression of human meibomian gland epithelial cells. Invest Ophthalmol Vis Sci 2013;54:2541–50. [PubMed: 23493293]

[11]. Liu Y, Ding J. The combined effect of azithromycin and insulin-like growth factor-1 on cultured human meibomian gland epithelial cells. Invest Ophthalmol Vis Sci 2014;55:5596–601. [PubMed: 25125598]

[12]. Butovich IA. Tear film lipids. Exp Eye Res 2013;117:4–27. [PubMed: 23769846]

[13]. Butovich IA, McMahon A, Wojtowicz JC, Lin F, Mancini R, Itani K. Dissecting lipid metabolism in meibomian glands of humans and mice: an integrative study reveals a network of metabolic reactions not duplicated in other tissues. Biochim Biophys Acta 2016;1861:538–53. [PubMed: 27032494]

[14]. Widjaja-Adhi MAK, Silvaroli JA, Chelstowska S, Trischman T, Bederman I, Sayegh R, et al. Deficiency in Acyl-CoA:Wax Alcohol Acyltransferase 2 causes evaporative dry eye disease by abolishing biosynthesis of wax esters. Faseb J 2020;34:13792–808. [PubMed: 32851726]

[15]. Sawai M, Watanabe K, Tanaka K, Kinoshita W, Otsuka K, Miyamoto M, et al. Diverse meibum lipids produced by Awat1 and Awat2 are important for stabilizing tear film and protecting the ocular surface. iScience 2021;24:102478. [PubMed: 34113821]

[16]. Parfitt GJ, Brown DJ, Jester JV. Transcriptome analysis of aging mouse meibomian glands. Mol Vis 2016;22:518–27. [PubMed: 27279727]

[17]. Kim SW, Brown DJ, Jester JV. Transcriptome analysis after PPARgamma activation in human meibomian gland epithelial cells (hMGEC). Ocul Surf 2019;17:809–16. [PubMed: 30742991]

[18]. Hampel U, Schroder A, Mitchell T, Brown S, Snikeris P, Garreis F, et al. Serum-induced keratinization processes in an immortalized human meibomian gland epithelial cell line. PLoS One 2015;10:e0128096. [PubMed: 26042605]

[19]. Ziemanski JF, Chen J, Nichols KK. Evaluation of cell harvesting techniques to optimize lipidomic analysis from human meibomian gland epithelial cells in culture. Int J Mol Sci 2020;21. [PubMed: 33375030]

[20]. Maskin SL, Tseng SC. Clonal growth and differentiation of rabbit meibomian gland epithelium in serum-free culture: differential modulation by EGF and FGF. Invest Ophthalmol Vis Sci 1992;33:205–17. [PubMed: 1370439]

[21]. Nicolaides N, Santos EC, Smith RE, Jester JV. Meibomian gland dysfunction. III. Meibomian gland lipids. Invest Ophthalmol Vis Sci 1989;30:946–51. [PubMed: 2498228]

[22]. Butovich IA, Lu H, McMahon A, Eule JC. Toward an animal model of the human tear film: biochemical comparison of the mouse, canine, rabbit, and human meibomian lipidomes. Invest Ophthalmol Vis Sci 2012;53:6881–96. [PubMed: 22918629]

[23]. Jester JV, Potma E, Brown DJ. PPARgamma regulates mouse meibocyte differentiation and lipid synthesis. Ocul Surf 2016;14:484–94. [PubMed: 27531629]

[24]. Butovich IA, Uchiyama E, Di Pascuale MA, McCulley JP. Liquid chromatography-mass spectrometric analysis of lipids present in human meibomian gland secretions. Lipids 2007;42:765–76. [PubMed: 17605062]

[25]. Vrkoslav V, Mikova R, Cvacka J. Characterization of natural wax esters by MALDI-TOF mass spectrometry. J Mass Spectrom 2009;44:101–10. [PubMed: 18821728]

[26]. Menzel-Severing J, Zenkel M, Polisetti N, Sock E, Wegner M, Kruse FE, et al. Transcription factor profiling identifies Sox9 as regulator of proliferation and differentiation in corneal epithelial stem/progenitor cells. Sci Rep 2018;8:10268. [PubMed: 29980721]

[27]. Pellegrini G, Dellambra E, Golisano O, Martinelli E, Fantozzi I, Bondanza S, et al. p63 identifies keratinocyte stem cells. Proc Natl Acad Sci U S A 2001;98:3156–61. [PubMed: 11248048]

[28]. Kim SW, Rho CR, Kim J, Xie Y, Prince RC, Mustafa K, et al. Eicosapentaenoic acid (EPA) activates PPARgamma signaling leading to cell cycle exit, lipid accumulation, and autophagy in human meibomian gland epithelial cells (hMGEC). Ocul Surf 2020;18:427–37. [PubMed: 32360782]

[29]. Kim SW, Xie Y, Nguyen PQ, Bui VT, Huynh K, Kang JS, et al. PPARgamma regulates meibocyte differentiation and lipid synthesis of cultured human meibomian gland epithelial cells (hMGEC). Ocul Surf 2018;16:463–9. [PubMed: 29990545]

[30]. Turkish AR, Henneberry AL, Cromley D, Padamsee M, Oelkers P, Bazzi H, et al. Identification of two novel human acyl-CoA wax alcohol acyltransferases: members of the diacylglycerol acyltransferase 2 (DGAT2) gene superfamily. J Biol Chem 2005;280:14755–64. [PubMed: 15671038]

[31]. Ding J, Kam WR, Dieckow J, Sullivan DA. The influence of 13-cis retinoic acid on human meibomian gland epithelial cells. Invest Ophthalmol Vis Sci 2013;54:4341–50. [PubMed: 23722388]

[32]. Hampel U, Kruger M, Kunnen C, Garreis F, Willcox M, Paulsen F. In vitro effects of docosahexaenoic and eicosapentaenoic acid on human meibomian gland epithelial cells. Exp Eye Res 2015;140:139–48. [PubMed: 26335632]

[33]. Jun I, Kim BR, Park SY, Lee H, Kim J, Kim EK, et al. Interleukin-4 stimulates lipogenesis in meibocytes by activating the STAT6/PPARgamma signaling pathway. Ocul Surf 2020;18:575–82. [PubMed: 32360783]

[34]. Ziemanski JF, Wilson L, Barnes S, Nichols KK. Saturation of cholesteryl esters produced by human meibomian gland epithelial cells after treatment with rosiglitazone. Ocul Surf 2021;20:39–47. [PubMed: 33248214]

[35]. Sahin A, Liu Y, Kam WR, Darabad RR, Sullivan DA. Dihydrotestosterone suppression of proinflammatory gene expression in human meibomian gland epithelial cells. Ocul Surf 2020;18:199–205. [PubMed: 32112874]

[36]. Kam WR, Liu Y, Ding J, Sullivan DA. Do cyclosporine A, an IL-1 receptor antagonist, uridine triphosphate, rebamipide, and/or bimatoprost regulate human meibomian gland epithelial cells? Invest Ophthalmol Vis Sci 2016;57:4287–94. [PubMed: 27552406]

[37]. Chapman S, McDermott DH, Shen K, Jang MK, McBride AA. The effect of Rho kinase inhibition on long-term keratinocyte proliferation is rapid and conditional. Stem Cell Res Ther 2014;5:60. [PubMed: 24774536]

[38]. McMullan R, Lax S, Robertson VH, Radford DJ, Broad S, Watt FM, et al. Keratinocyte differentiation is regulated by the Rho and ROCK signaling pathway. Curr Biol 2003;13:2185–9. [PubMed: 14680635]

[39]. Strudwick XL, Lang DL, Smith LE, Cowin AJ. Combination of low calcium with Y-27632 rock inhibitor increases the proliferative capacity, expansion potential and lifespan of primary human keratinocytes while retaining their capacity to differentiate into stratified epidermis in a 3D skin model. PLoS One 2015;10:e0123651. [PubMed: 25874771]

[40]. Hennings H, Michael D, Cheng C, Steinert P, Holbrook K, Yuspa SH. Calcium regulation of growth and differentiation of mouse epidermal cells in culture. Cell 1980;19:245–54. [PubMed: 6153576]

[41]. Hampel U, Garreis F. The human meibomian gland epithelial cell line as a model to study meibomian gland dysfunction. Exp Eye Res 2017;163:46–52. [PubMed: 28363775]

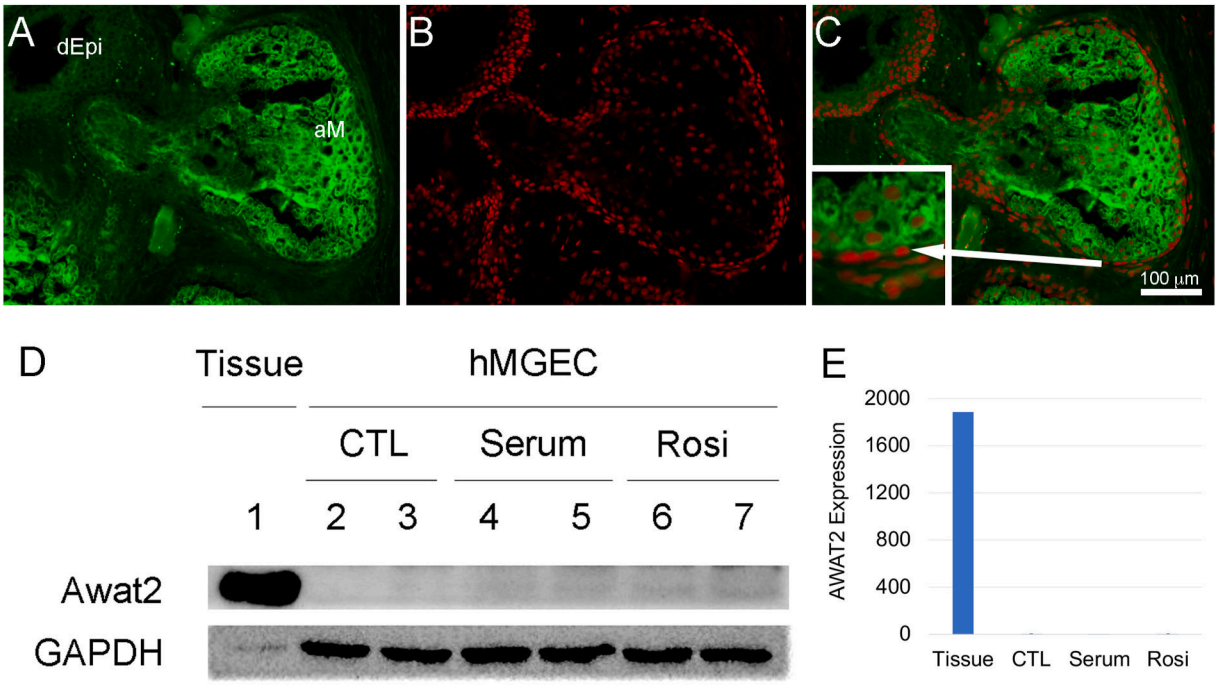

Fig. 1.

AWAT2 localization and expression in human eyelid tissue and cultured hMGEC. Immunolocalization of AWAT2 (Green) showed intense staining in acinar meibocytes (aM) compared to meibomian gland ductal epithelium (dEpi) and other tarsal tissue (A). Co-localization with nuclei (B, Red) showed AWAT2 localization restricted to the suprabasal acinar meibocytes with little or no staining of basal acinar cells or progenitor meibocytes (C, inset. Arrow indicates region shown in inset). Extraction of protein from the tarsal plate also showed very high expression in eyelid tissue (D, lane 1), while protein extracts from cultured hMGEC under control (CTL, lanes 2 and 3) or differentiation using DMEM/F12 with either serum (Serum, lanes 4 and 5) or rosiglitazone (Rosi, lanes 6 and 7) contained undetectable levels. qPCR (E) also showed very high expression of AWAT2 transcripts in human eyelid tissue (Tissue) compared to cultured hMGEC under control (CTL), Serum or rosiglitazone (Rosi) treatment when normalized to GAPDH.

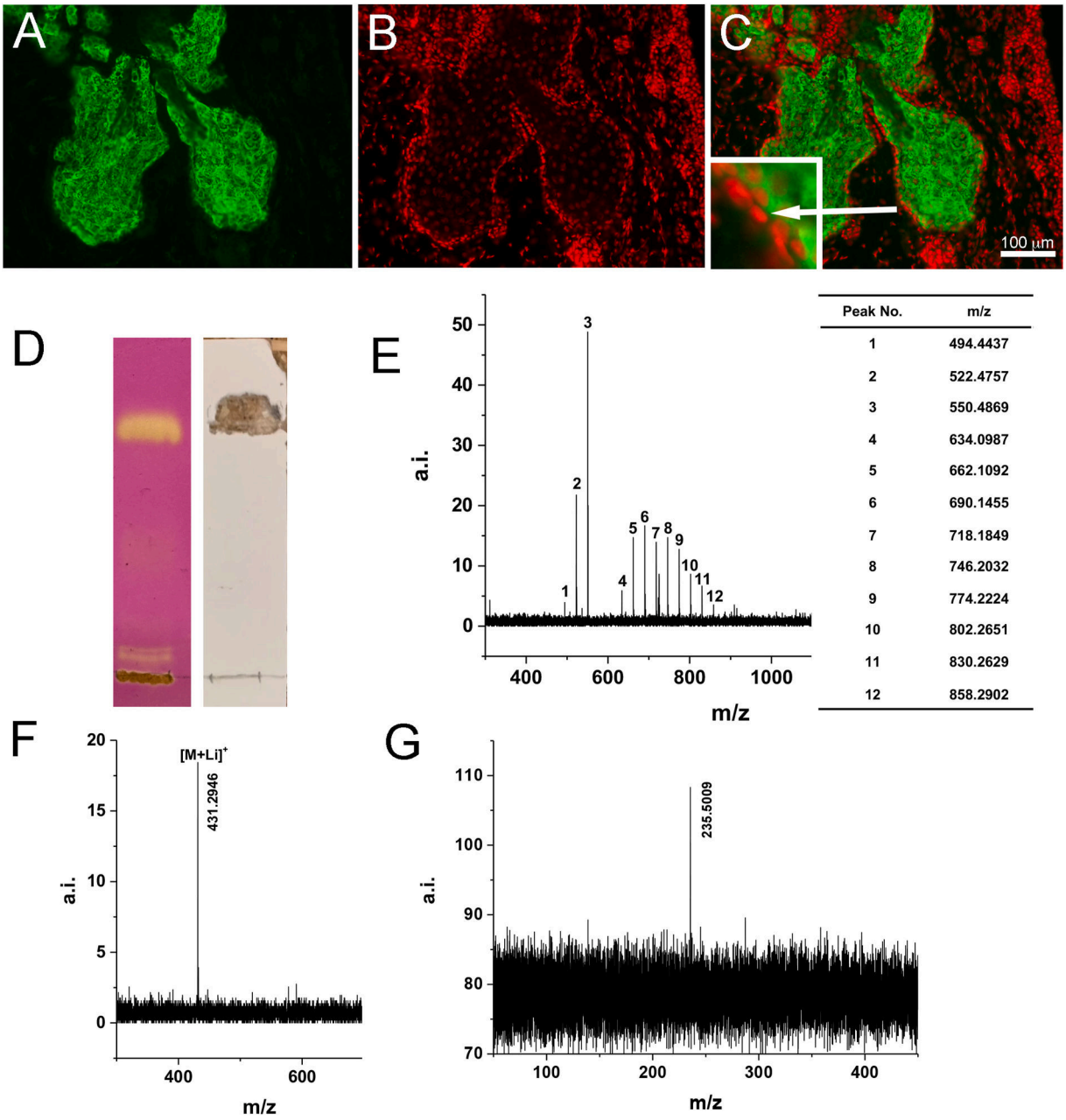

Peak No.	m/z
1	494.4437
2	522.4757
3	550.4869
4	634.0987
5	662.1092
6	690.1455
7	718.1849
8	746.2032
9	774.2224
10	802.2651
11	830.2629
12	858.2902

Fig. 2.

Immunolocalization of AWAT2 and characterization of wax esters in rabbit meibomian glands. AWAT2 (A, Green) and nuclear (B, Red) staining of rabbit eyelid tissue showed high expression in the meibomian acinar tissue that appear limited to the suprabasal acinar meibocytes (C) with little detectable staining in basal progenitor acinar cells (C, inset; arrow indicates region shown in inset) (D) Separation of meibomian gland lipids on TLC plates (the left plate was stained with iodine vapor to confirm the Rf of wax esters and wax esters were scraped from the unstained, right plate). (E) MALDI spectrum of WEs from meibomian gland measured in KDHB matrix. (F) MALDI spectrum showing the lithium adduct of myristyl myristate 14:0–14:0 (FW 424.7). G. MS/MS spectrum showing the only

fragment from myristyl myristate 14:0–14:0. The fragment (*m/z* 235.5) was identified as lithium adduct of tetradecanoic acid, which is the fatty acid part of myristyl myristate.

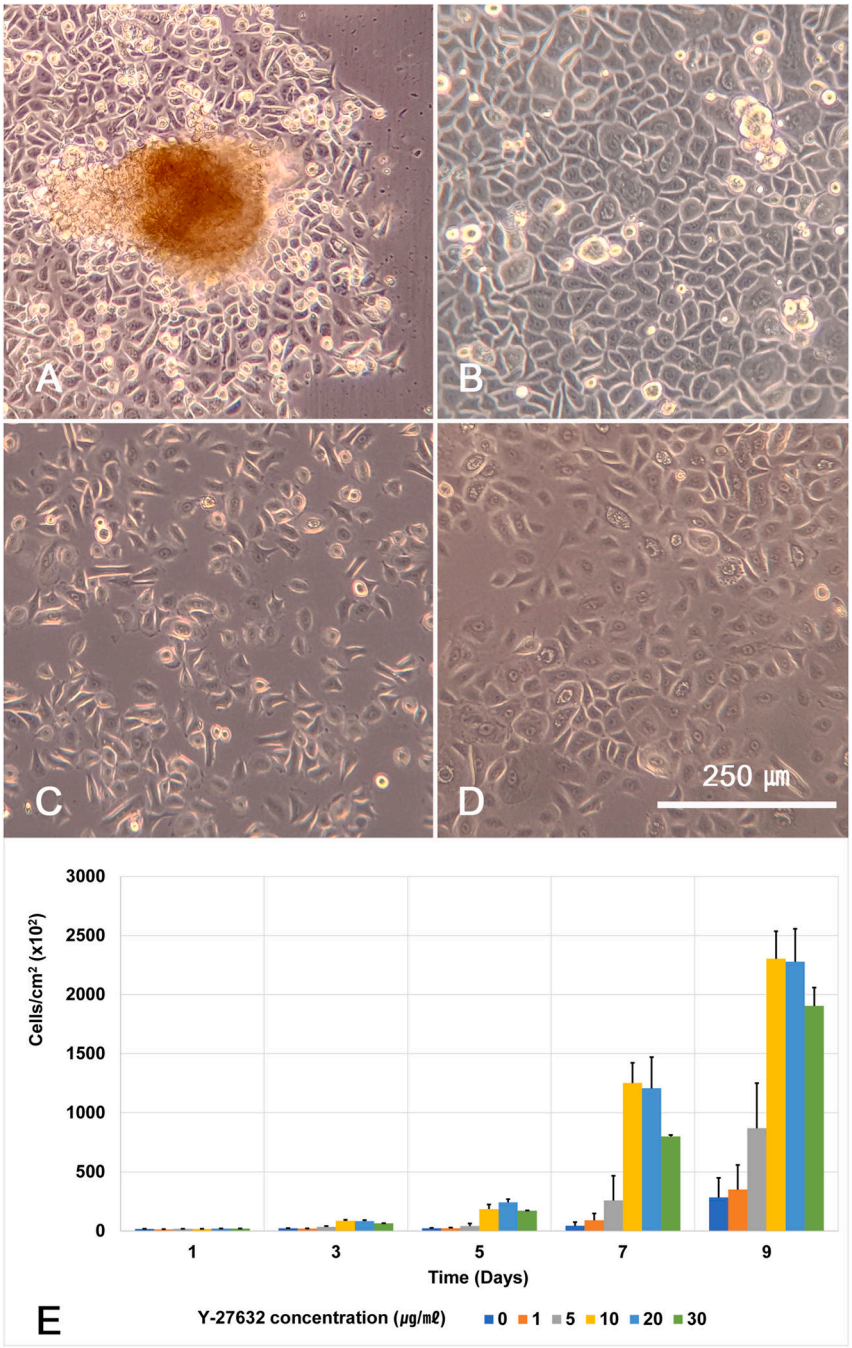

Fig. 3.

Phase microscopy (A–D) of different passages of rabbit rMPCs and growth kinetics (E) with different concentration of the ROCK inhibitor, Y-27632. (A) Primary rMPCs, note that cells are growing out from the isolated acini. rMPC at P1, P5, and P7 passage (B-D, respectively). Note that passaged cells maintained a polygonal epithelial morphology. (E) P2 cell growth in different Y-27632 concentrations. The growth was most rapid at 10 and 20 µM of Y-27632.

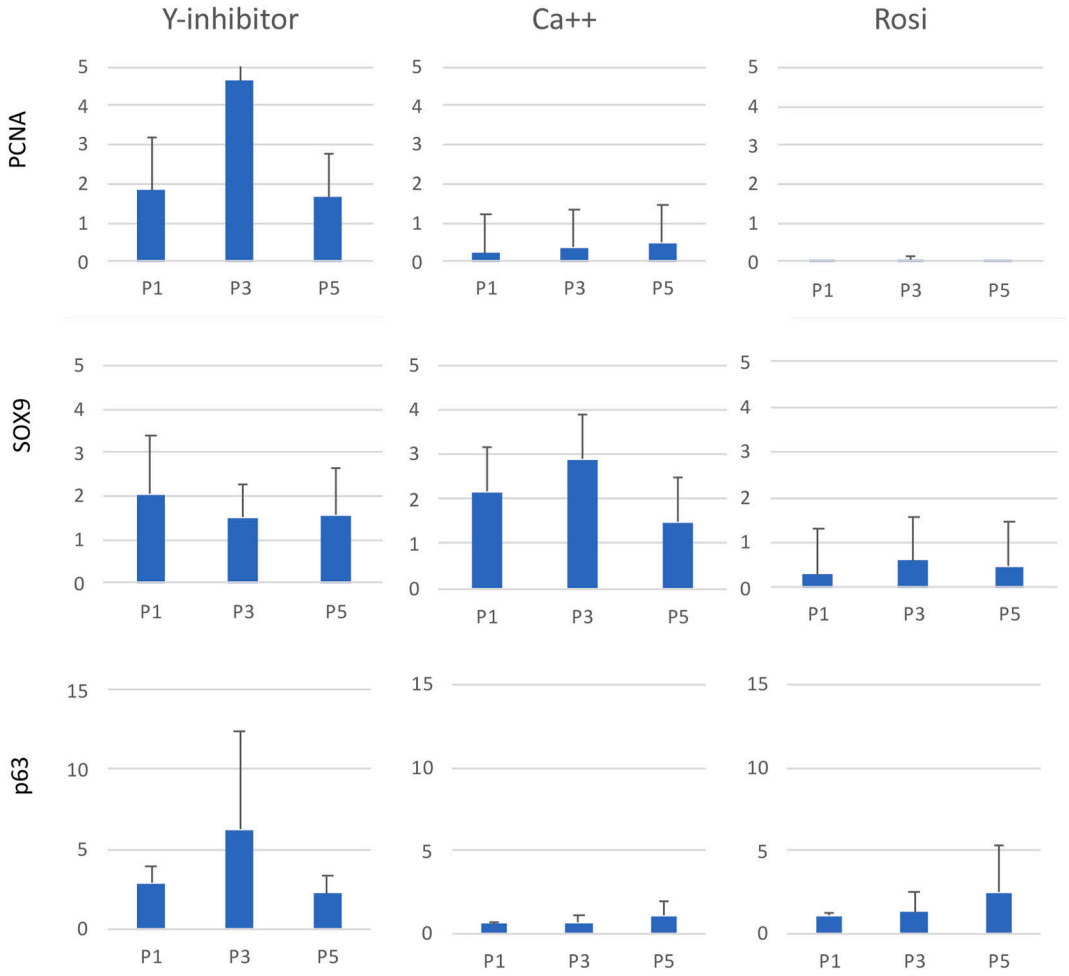

Fig. 4.

Effect of different media conditions on PCNA, SOX9 and p63 protein expression at P1, P3, and P5. Note that cells grown in CnT-BM.1 media with low calcium and the ROCK inhibitor, Y-27632 showed significantly elevated levels of PCNA, SOX9, and p63 indicating maintenance of a progenitor cell phenotype. Removal of the Y-27632 and the addition of calcium (1.0 mM) markedly reduced expression of both PCNA and p63. Addition of rosiglitazone to the calcium containing media further reduced PCNA expression as well as SOX9 expression.

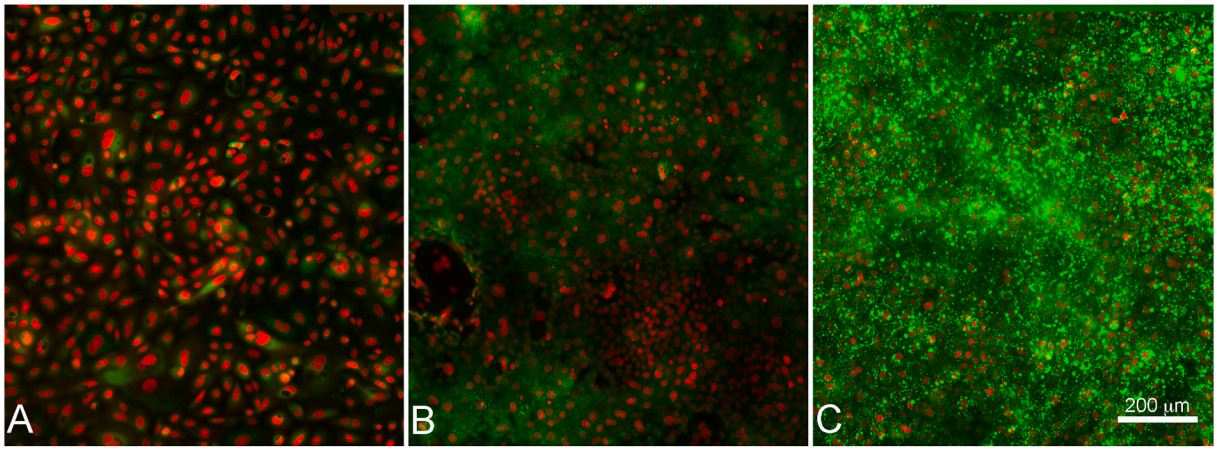

Fig. 5.

Lipid accumulation by rMPC and differentiated rMC. rMPC were plated on collagen coated glass coverslips and then cultured with either the progenitor cell growth media (A) or differentiation media containing high calcium and no Y-27632 without (B) and with rosiglitazone (C). Cells were cultured for 7 days and then fixed and stained for neutral lipid accumulation using LipidTox (Green) with counter staining for nuclei (Red). Note that lipid accumulation was only detected when cells were induced to synthesize lipid using the PPARγ.

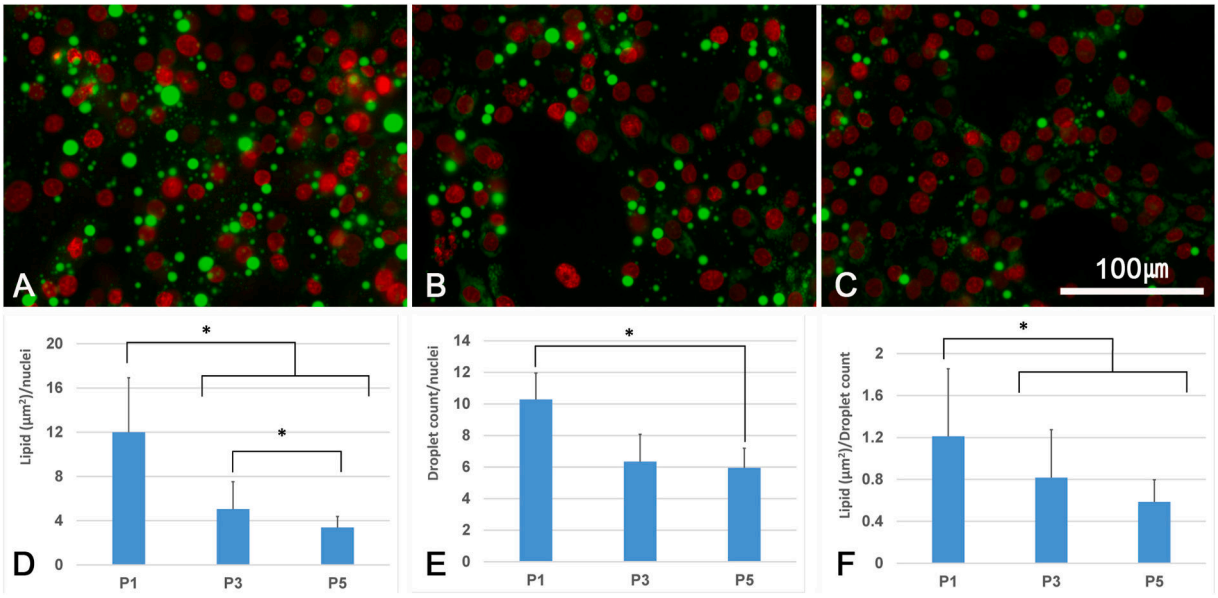

Fig. 6.

Effect of rMPC passage on lipid accumulation induced by rosiglitazone. P1 (A), P3 (B), and P5 (C) rMPC were platted onto glass coverslips and then induced to differentiate with rosiglitazone for 7 days. Cells were then stained with LipidTox to identify neutral lipid accumulation. All passage cells showed a significant increase of lipid droplets (A–C). Bar graphs (D) show lipid area (μm^2) per nuclei, (E) droplet count per nuclei, and (F) lipid area (μm^2) per droplet count. While lipid droplets were present at all passages, there appeared to be a general decrease in the lipid droplet area/cell, number, and size with passage.

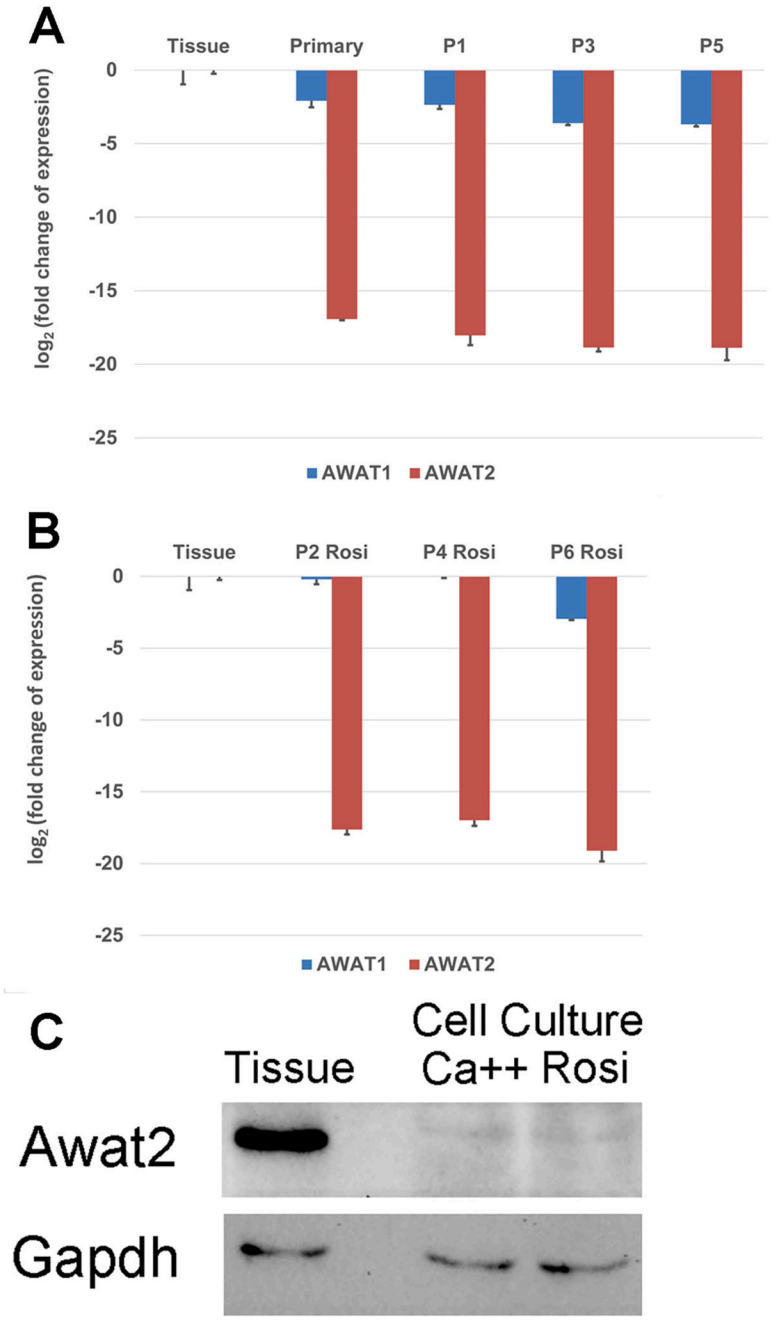

Fig. 7.

Effect of passage and differentiation on mRNA expression of AWAT1 and AWAT2. (A) Compared to tissue AWAT2 mRNA expression level, the mRNA extracted from cultured rMPCs decreased dramatically and was barely detectible even in primary cultured rMPC. The decrease was less evident for AWAT1 mRNA. (B) Differentiation of rMPCs to rMCs with rosiglitazone failed to show any substantial increase in the expression of AWAT2. By comparison, AWAT1 mRNA increased to almost tissue levels in P2 and P4 cells, but the effect disappeared in P6. These RNA results were further confirmed by western blotting (C)

which showed barely detectible levels of AWAT2 in protein extracts for rMCs differentiated with just calcium (Ca++) or rosiglitazone (Rosi) compared to tissue AWAT2 levels.

Table 1

PCR primers designed for human and rabbit RNA. Accession number (NVBI Reference Sequence), sequences and product length are summarized. F *forward,* R *reverse.*

Gene		Accession number	Primer sequence (5’ - 3’)	Product length
Human	AWAT2	NG_021246.1 (h)	F-AAGATATTTCCTGGCATCAC R-CCCCTGTAGACATTACATATTC	91 bp
	GAPDH	NG_007073.2 (h)	F-ACAGTTGCCATGTAGACC R-TTGAGACACGGGTACTTTA	88 bp
Rabbit	AWAT1	XM_002720072.3 (rb)	F- TGTTCCAAGCGGCGTAATCA R- GTGACCTCGGTGCAGAAGTT	356 bp
	AWAT2	XM_002720065.3 (rb)	F- TGGTGGTGTTTACGCCCTAC R- GTGTTTCCACAAGCGCCATT	128 bp
	AWAT2–3	XM_002720065.3 (rb)	F-CCACGTCTACCCTTGTGCTT R-CACGACTGGCCAAGTTAGGT	340 bp
	Actin	NM_ 001101683.1 (rb)	F-ATCGTGATGGACTCCGGCGAC R-AGCGCCACGTAGCACAGC	212 bp
	GAPDH	NM_001082253.1 (rb)	F- GAGCTGAACGGGAAACTCAC R- CCCTGTTGCTGTAGCCAAAT	304 bp